Investigation on Medium-Term Performances of Porous Asphalt and Their Impacts on Tire/Pavement Noise

Hao Wu , Ge Wang , Ming Liang Li * , Yue Zhao , Jun Li , Ding Ding Han , Peng Fei Li *

Posted Date: 7 December 2023

doi: 10.20944/preprints202312.0490.v1

Keywords: Porous asphalt pavement; OBSI; Road performance degradation; Correlation; Tire/pavement noise

Article

Investigation on Medium-Term Performances of Porous Asphalt and Their Impacts on Tire/Pavement Noise

Hao Wu [1], Ge Wang [2], Mingliang Li [1,*], Yue Zhao [2], Jun Li [1], Dingding Han [1] and Pengfei Li [3,*]

[1] Key Laboratory of Transport Industry of Road Structure and Material, Research Institute of Highway Ministry of Transport, Xitucheng Road No. 8, Beijing 100088, China.
[2] Jiangsu Expressway Engineering Maintenance Limited Company, Shantou Road No. 2, Huai'an, Jiangsu Province, 223000, China.
[3] School of Civil and Transportation Engineering, Beijing University of Civil Engineering and Architecture, Beijing 100044, China.
* Correspondence: ml.li@rioh.cn; lzppercy_2012@163.com; Tel.: +86+010-62079235

Abstract: As the lifespan of porous asphalt pavement extends, it invariably experiences performance degradation and an increase in tire/pavement noise compared with the original surface when it is newly built. To understand the medium-term performance of porous asphalt pavement during service and reveal the influence of different pavement performance indicators on tire/pavement noise generation, a seven-year continuous observation and data analysis study was conducted. Porous asphalt with different designed material parameters was taken into account, including thin-layer porous asphalt overlay with a maximum nominal aggregate size of 10mm (PUC-10), porous asphalt with a maximum nominal aggregate size of 13mm (PAC-13), and a two-layer porous asphalt incorporating both PUC-10 and PAC-13 (PUC-10+PAC-13). Using automated pavement technology testing equipment, key performance indexes, including damage rate (DR), rut depth (RD), international roughness index (IRI), and sideway force coefficient (SFC), were measured and calculated. The on-board sound intensity (OBSI) method was used to test noise levels in three types of porous asphalt pavement structures and on a dense graded easy compact asphalt concrete (ECA) for comparison. The progressions of the medium-term performances were analyzed according to the measured results. The correlations between tire/pavement noise levels and testing speed, testing lane, pavement structure, and road condition indicators were investigated by regression. The research results revealed that the DR and SFC of the three types of porous asphalt pavement displayed more significant attenuation in the service period, while the IRI and RD showed small changes. Among them, the SFC demonstrated significant attenuation over the first 4 years, decreasing between 13.8% and 17.0%. From the 3-7 years of operation, the transverse crack disease in porous asphalt pavement progressed rapidly. The three porous asphalt pavement structures tested exhibited commendable noise reduction capabilities. Compared to ECA, the OBSI noise levels of these structures were lower by 2.09 dB, 1.53 dB, and 2.88 dB, respectively. Compared to other pavement condition indicators, RD had a more significant impact on the OBSI value of the PUC-10 porous asphalt pavement. For the PUC-10+PAC-13 porous asphalt pavement, there was a significant linear relationship between the OBSI value and SFC, mainly due to polishing of the coarse aggregate surface. It leads to a decrease of the micro-texture, which lies in increasing tire/pavement noise at high-frequency ranges and decreasing SFC. This study will have guiding significance for the research of the attenuated law and durability improvement of porous asphalt tire/pavement noise.

Keywords: porous asphalt pavement; Tire/pavement noise; OBSI; Road performance degradation; Correlation

 doi:10.20944/preprints202312.0490.v1

1. Introduction

With good drainage and noise reduction characteristics, porous asphalt is commonly used for safety improvement and traffic noise mitigation [1–5]. Affected by factors such as vehicle loading, environment, diseases will gradually appear and develop. Raveling is the typical disease of porous asphalt pavements [6]. When coarse aggregates are stripped off from the surface, there will be changes in the surface texture at the macro level, which leads to an increasein the vibration of rolling on the pavement. Therefore, the noise emission level between the tire and pavement is also increased according to the generation mechanisms of tire/pavement noise, especially for the noise in the low-frequency ranges (500~800Hz) [7].

Tire/pavement noise varies with aggregate type, gradation, asphalt and porosity, and density of asphalt mixture of the pavement [8–10]. There is a particular linear relationship between the gradation of the low-noise asphalt pavement, the porosity of the mixture, the construction depth, and the noise value of the close proximity method (CPX) [11,12]. Tires with different tread patterns and structures will generate various levels and frequencies of noise on the same pavement [13]. The maximum tire/pavement noise is typically between 800 Hz and 1200 Hz [14]. Many studies have revealed that porosity is the most critical factor for the noise reduction of porous asphalt, followed by the surface texture depth and mechanical impedance [15]. The aggregate particle size also significantly impacts the noise reduction performance, and 9.5 mm particles show the greatest effect, followed by 1.18 mm and 2.36 mm particles. Thinner porous asphalt layers using finer aggregate generally have a higher peak frequency of the noise absorption coefficient and vice versa [16]. Adding materials such as plastic and rubber in a certain proportion to the asphalt pavement can effectively improve the noise reduction performance of the asphalt pavement by changing the mechanical impedance [17,18].

The porosity of the asphalt mixture can be obtained using CT scanning and X-ray tomography, thus acquiring the microscopic characteristics of the asphalt mixture, the degradation law of the porosity, and the noise absorption coefficient of the mixture [19–24]. The relationship between the length of the connected pores and the pavement thickness can be quantified through the effect of airflow velocity on the flow resistance and the measured spectrum of the noise absorption coefficient. By improving the Zwikiker-Kosten model in combination with the indoor test of the noise absorption coefficient of the asphalt mixture, the noise absorption performance of the porous asphalt mixture can be predicted [25]. Methods such as the surface texture level of the mixture, tire-dropping method, and pendulum test can effectively predict the tire/pavement noise of porous asphalt pavement [26]. With the influences of pavement aging, vehicle load, and environmental effects, the pores of porous asphalt pavement will be gradually blocked, resulting in a change in noise absorption frequency and a significant reduction in noise absorption performance [27].

In China, the service performance of pavement in use is mainly evaluated by the pavement quality index (PQI). PQI is calculated from indicators including pavement condition index (PCI), riding quality index (RQI), rutting depth index (RDI), pavement wear index (PWI), and skidding resistance index (SRI), and these indicators are considered as references for pavement maintenance decision-making [28–33]. However, no special indicator reflects the raveling of porous asphalt pavements. Rapid and non-destructive recognition of raveling is necessary for the decision-making on maintaining porous asphalt pavements. Data collection and automatic methods are available to detect asphalt pavement macrostructures based on tire/pavement noise signals [34].

Before 2015, the application of porous asphalt pavement in China was relatively limited. However, after 2014, with the adoption of expressway maintenance projects in provinces like Jiangsu Province, Hunan Province, etc., porous asphalt became popular due to its safety and environment-friendly characteristics. In order to fully study the performance changes of actual porous asphalt pavement in use in China, continuous pavement performance measurements, including DR, RD, IRI, SFC,were carried out for 7 years, and tire/pavement noise data were also collected in 2022. Consequently, medium-term performance variation tendencies of porous asphalt pavement were obtained. Correlations between performance indicators and noise level values were investigated, and possibility of using tire/pavement noise level for evaluation of ravelinug damage of porous asphalt pavement was explored in this way. The research revealed a medium-term performance of using

Preprints (www.preprints.org) | NOT PEER-REVIEWED | Posted: 7 December 2023 doi:10.20944/preprints202312.0490.v1

porous asphalt in maintenance engineering, and it contributed to a deeper understanding of the causes of tire/pavement noise changes.

2. Test Sections and Methods

2.1. Test Sections

This study was performed based on the pavement engineering of the Yancheng-Jingjiang Expressway in Jiangsu Province, China, a two-way 4-lane highway. The engineering section was located in the downstream direction K162+700-K157+000, with a length of about 5.7 km. In the tested section, there were four types of asphalt pavement structures: (1) Easy compact asphalt (ECA) concrete was used as the top layer, with SMA-13/AC-20/AC-25 asphalt mixture courses underneath in order. (2) Thin-layer porous asphalt overlay with a maximum nominal aggregate size of 10mm (PUC-10) was paved as the top layer, and SMA-13/AC-20/AC-25 asphalt layers underneath were in order. (3) Porous asphalt with a maximum nominal aggregate size of 13mm (PAC-13), with AK-13/AC-20/AC-25 asphalt layers underneath in order. (4) Two-layer porous asphalt with PUC-10+PUC-13, with AC-20/AC-25 asphalt layers underneath in order. Schemes of those pavement structures are shown in Figure 1, with thickness for each layer of different structures. Porous asphalt mixtures are shown in Figure 2.

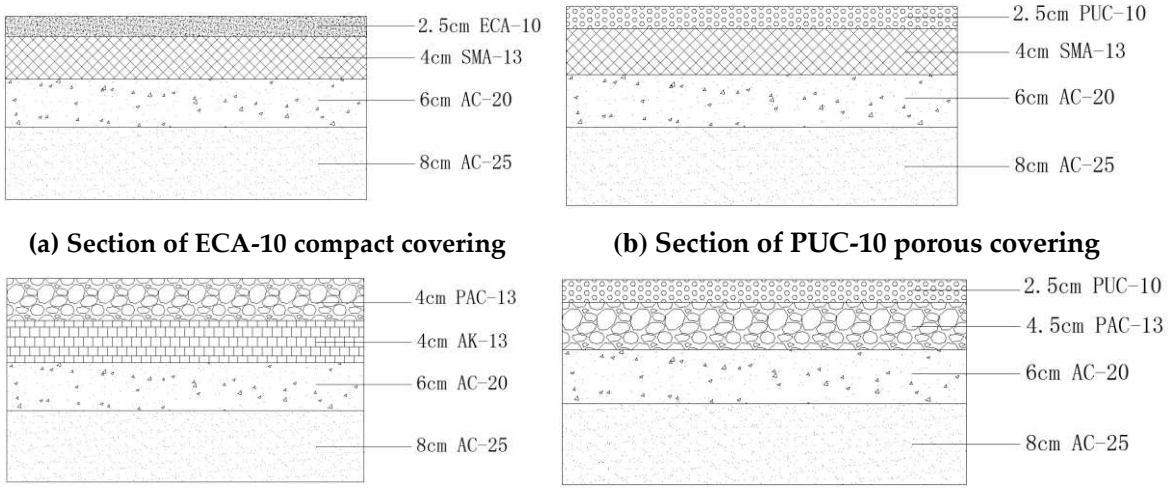

(a) Section of ECA-10 compact covering **(b) Section of PUC-10 porous covering**

(c) Section of PAC-13 porous pavement surface **(d) Section of PUC-10+PAC-13 porous pavement surface**

Figure 1. Diagram of pavement structures.

(a)) PUC-10 (10~30mm) **(b) PAC-13 (40~50mm)** **(c) PUC-10+PAC-13 (20~40mm+35~60mm)**

Figure 2. Porous asphalt mixtures.

Preprints (www.preprints.org) | NOT PEER-REVIEWED | Posted: 7 December 2023 doi:10.20944/preprints202312.0490.v1

To understand the medium-term service performance of porous asphalt and determine influence of service property of porous asphalt on tire/pavement noise, the service performance indicators of porous asphalt were tracked and observed continuously for 7 years, namely from 2015 to 2022.According to the "*Highway Performance Assessment Standards*" (JTG 5210-2018), *Multifunctional High-Speed Highway Condition Monitor* (GB/T 26764) and *Specifications of Automated Pavement Condition Survey* (JTG/T E61-2014) of China, cracking and other information collecting system (CiCS) of multifunctional automatic pavement detection vehicle and friction coefficient meter were used as automatic detection equipments to detect the indicators of DR, RD, IRI, SFC, and sensor measured texture depth (SMTD). The tire/pavement noise data were also collected by OBSI test in 2022.

According to the *Standard Test Methods of Bitumen and Bituminous Mixtures for Highway Engineering* (JTG E20-2011) of China, the characteristics of different road surface mixtures were measured. The gradation and performance indicators of asphalt mixture on the pavement surface are shown in Table 1 and Table 2, respectively. Among the four pavement structures, the biggest difference lies in the gradation and porosity of the surface asphalt mixture, which lead to various performances between mixtures.

Table 1. Designed gradations of different asphalt mixtures.

Type of mixture	Passing percentage (%) of the following sieve holes (mm)												Polyester fiber content (%)	Asphalt-aggregate ration (%)
	16.0	13.2	9.5	7.5	6.7	4.75	2.36	1.18	0.6	0.3	0.15	0.075		
ECA-10	100	100	92.7	-	44.9	28.8	23.4	17.1	11.1	8.9	8	6.4	0.2	5.4
PUC-10	100	100	90.0	72.0	-	25.3	12.3	11.9	9.1	7.5	6.4	5.4	0.1	5.0
PAC-13	100	87.5	4.8	-	-	13.7	11.2	8.7	7.3	6.2	5.4	4.8	0.1	4.8

Table 2. Performances of different asphalt mixtures.

Indicator Name	Unit	ECA-10	PUC-10	PAC-13
Void content percentage	%	4.2	20.4	19.9
Marshall Stability	kN	9.1	7.22	7.42
Residual Mashall stability percentage	%	94.6	90.4	89.7
Residual Freeze-thaw split tensile strength ratio	%	93.4	95.7	84.8
Standard raveling loss percentage	%	3.32	5.3	7.5
Immersion raveling loss percentage	%	-	4.3	9.2
Dynamic Stability	time/mm	5231	6574	9043
Permeability	ml/min	52	6570	7116

2.2. Test Methods

2.2.1. CiCS of Multifunctional Automatic Pavement Detection Vehicle

The CiCS of multifunctional automatic pavement detection vehicle is road surface detection equipment independently developed by our institute, shown in Figure 3. It passed the SCANNER certification organized by the Transport Research Institute in the UK in 2012, which can output 40 road condition indicators, including DR, RD, IRI, SFC, SMTD and etc. The effective detection speed

 doi:10.20944/preprints202312.0490.v1

is 0~100km/h. The frequency of the sensor is 20kHz/s. The coefficient of variation is 1.6%~3.6%, and its correlation is 0.992~0.998.

Figure 3. CiCS vehicle.

2.2.2. On-board Sound Intensity (OBSI) Tire/Pavement Noise Test

According to the American Association of State Highway and Transportation Officials (AASHTO) standard (T 360-16), the noise of the section was tested with the OBSI method. The test vehicle was a light passenger car, and the standard reference test tires (SRTT) were utilized. A pair of sound intensity sensors were arranged at both the front and rear ends of the tires. The distance of the sensor from the tire sidewall was 101.6 mm, and the height from the pavement surface was 76.2 mm. The two sensors were arranged symmetrically on both sides of the center line of the tire axle, with a horizontal distance of 209.6 mm and a standard speed of 97 km/h during the test. The device is shown in Figure 4. The noise intensity of different lanes, different pavement structures as given in Figure 1 were measured.


S

Figure 4. OBSI measurement equipment.

 doi:10.20944/preprints202312.0490.v1

2.3. Characteristic Indexes

IRI is an important indicator in pavement design, construction acceptance, and maintenance, which reflects the comfort of drivers and passengers and the safety and durability of the pavement. Vehicles traveling on rough pavements will generate additional vibrations, accelerating damage to vehicles and pavements. The higher the IRI was, the worse the smoothness of the pavement surface was. The IRI was detected and analyzed by the CiCS vehicle. The longitudinal section data on the tire tracks were continuously measured by the high-speed laser rangefinder and the accelerometer, and the data errors caused by vehicle bumps were effectively eliminated by the self-developed inertia compensation scheme. The resolution of the laser sensor is 0.05mm. With the support of the positioning data of the integrated control system, the IRI was obtained in real-time through the on-board data acquisition and processing software.

RD is for evaluating road performance. Rutting is a form of damage to asphalt pavement, manifested as a concave surface within the range of the asphalt pavement wheel track, sometimes accompanied by a raised edge of the wheel track. The deeper the RD was, the stronger the bumpiness and vibration of the car during driving. It will impact the vibration noise of the road surface/tires. The RD was detected and analyzed by the CiCS vehicle. Based on the high-resolution and high-frequency sampling frequency of the sensor camera and the sub-pixel data analysis algorithm, the laser image rutting meter was applied to acquire pavement cross-section curves at a fixed sampling interval and calculate the pavement RD values by matching the rutting model to the acquired pavement curves.

SFC is an indicator that characterizes the anti-sliding performance of pavements, directly related to the safety of driving, and is a key quality control indicator during the construction and operation of highways. The SFC was detected and analyzed by the Mu-Meter MK6 friction coefficient meter. Continuous and uninterrupted detection ensured a certain thickness of water film on the pavement surface. An SFC value was output every 10 m, with a detection speed of 50 km/h. The MK6 used the sophisticated tilting tire principle to measure the loads generated by the tires as they passed over the pavement surface, with the tire at an angle of 7.5° to the direction of travel.

DR was detected and analyzed by the CiCS vehicle. The two-dimensional pavement damage detection system was mainly used to detect and recognize pavement diseases. The damage to the road surface can significantly impact the vibration and noise of the road surface/tires.

SMTD was detected and analyzed by the CiCS vehicle. The three-line construction depth was obtained through the pavement wear detection system by adding one laser rangefinder at the left, middle, and right positions behind the vehicle platform (the rangefinders at the left and right positions were shared with the roughness system).

According to the industrial standards of "*Highway Performance Assessment Standards*" (JTG5210-2018) of China, the values of the indicators DR, RD, IRI, and SFC were converted into the PCI, RDI, RQI, and SRI. The calculation formulas are as follows.

(1) PCI

The value of PCI ranged from 0 to 100, and a greater value represented a better pavement condition. The calculation formula of PCI is given as follow:

$$PCI = 100 - a_0 DR^{a_1} \quad (1)$$

The DR of asphalt pavement was calculated based on the following formula:

$$\mathrm{DR} = 100 \times \frac{\sum_{i=1}^{i_0} W_i A_i}{A} \quad (2)$$

Where, DR means the percentage (%) of the sum of the converted areas of various pavement damages to the area of surveyed pavement;

A_i - area of damaged pavement of type i (m^2);

A - area of surveyed pavement (the product of the surveyed length and the effective pavement width) (m^2);

w_i - weight of the pavement damage of type i, referring to the corresponding specification;

i- individual type of damage in item i considering the degree of damage (mild, moderate, and severe);

Preprints (www.preprints.org) | NOT PEER-REVIEWED | Posted: 7 December 2023 doi:10.20944/preprints202312.0490.v1

a_0 and a_1 are constants, for expressways, a_0=15.00, a_1=0.412.

(2) RDI

The value of pavement RDI ranged from 0 to 100, and a greater value represented a better pavement condition. The relationship between RDI and RD is as follows:

$$RDI = \begin{cases} 100 - RD, & RD \le RD_a \\ 90 - 3 \bullet (RD - RD_a), & RD_a < RD \le RD_b \\ 0 & RD > RD_b \end{cases} \quad (3)$$

Where, RD_a=10.0, RD_b=40.0

(3) RQI

The RQI is calculated based on the formula below:

$$\text{RQI} = \frac{100}{1+a_2 e^{a_3 IRI}} \quad (4)$$

Where a_2 and a_3 are constants, for expressways, a_2=15.00, a_3=0.412.

(4)SRI

$$SRI = \frac{100-SRI_{min}}{1+b_0 e^{b_1 SFC_{min}}} \quad (5)$$

Where, SRI_{min}=35.0, b_0= 28.8, b_1= -0.105

(5) TCS

The total number of transverse cracks in the detected section was recorded, and the average value of the transverse crack spacing (TCS) per kilometer was obtained by:

$$TCS = \frac{1{,}000}{n+1} \quad (6)$$

Where, n is total number of transverse cracks in the detected section

3. Result and Analysis

3.1. Development Trend of Service Performance of Porous Asphalt Pavement

The service performance indicators of the three porous pavement structures (PUC-10/PAC-13/PUC-10+PAC-13) were measured by years. The measurement results are shown in Figure 5.

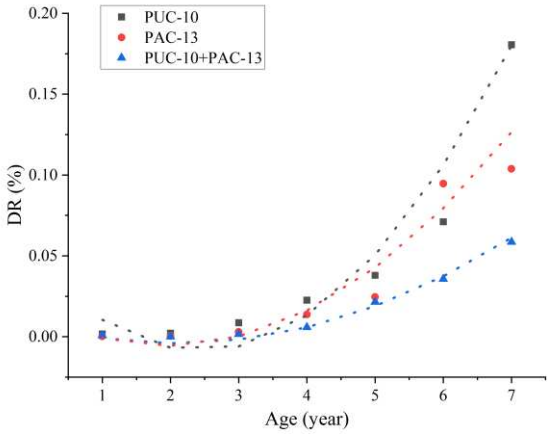

(**a**) DR

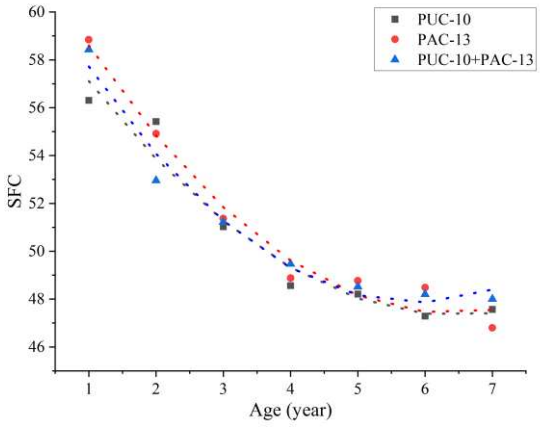

(**b**) SFC

Preprints (www.preprints.org) | NOT PEER-REVIEWED | Posted: 7 December 2023 doi:10.20944/preprints202312.0490.v1

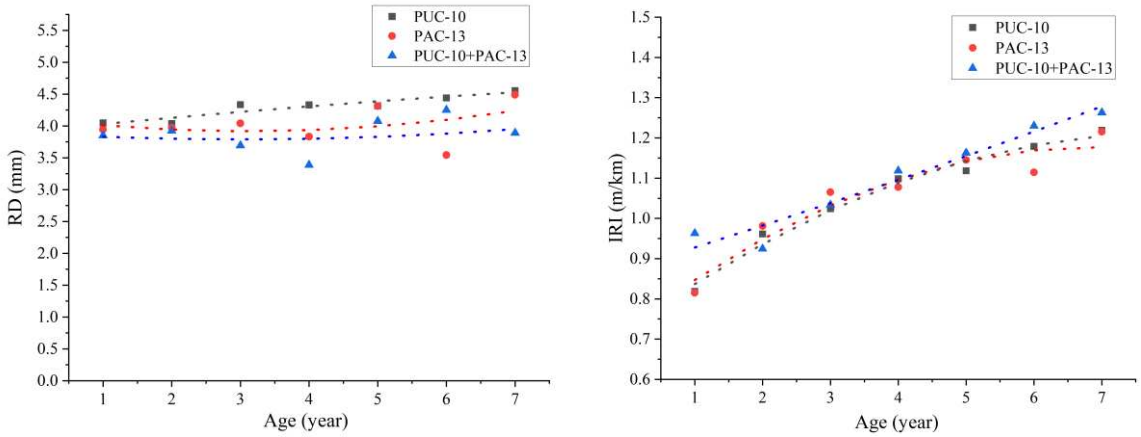

(c) RD (d) IRI

Figure 5. Changes of pavement condition indicators with years of operation.

According to Figure 5, different pavement structures exhibited various characteristics of pavement service performance. The DR of the three porous pavement structures increased to a certain extent with time, and the DR of PUC-10, PAC-13, and PUC-10+PAC-13 remained higher after 7 years of application. The proportions of different type of damage diseases are plotted in Figure 6. It indicats that the transverse crack disease is the main damage disease type of porous asphalt, accounting for about 77% . The TCS results and the typical of porous pavement diseases are shown in Figure 7 to Figure 8. It is found that after three years of construction, the crack spacing of each pavement structure was greatly reduced, indicating that the transverse crack of the porous asphalt developed rapidly after three years of operation. It is the main reason for the increase of DR.

During the 1-4 years of operation, the SFC of the three porous pavement structures decreased greatly, with an SFC decay rate of 13.8-17.0%, meaning the SFC value's reuction rate was relatively slight after 4 years of operation. The RD of the three porous asphalt pavement structures did not decay significantly during the 7 years of operation, suggesting that the porous asphalt pavement has excellent anti-rutting performance. IRI did not decay obviously, and the IRI of PUC-10, PAC-13, and PUC-10+PAC-13 reached 1.22-1.26 m/km, which was mainly due to the rapid development of transverse crack disease with years, resulting in the IRI decay to some degree.

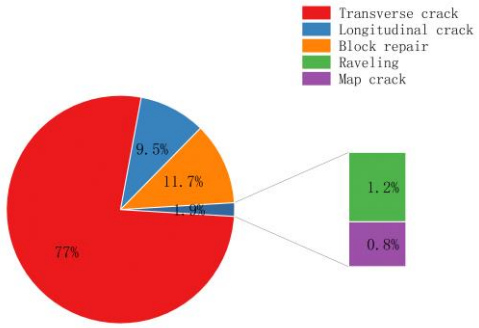

Figure 6. The proportion of pavement disease by types.

Preprints (www.preprints.org) | NOT PEER-REVIEWED | Posted: 7 December 2023 doi:10.20944/preprints202312.0490.v1

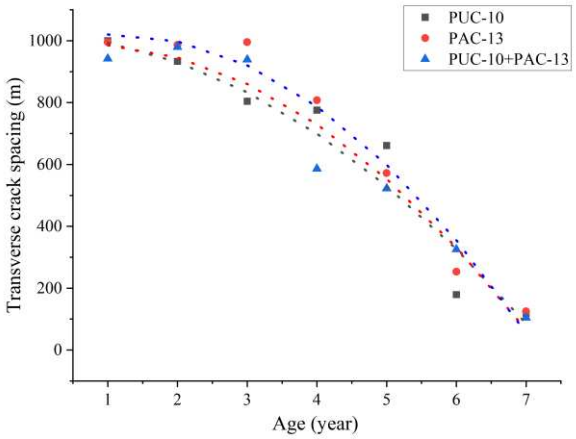

Figure 7. The change of crack spacing with the years of operation.

(**a**)Transverse crack (**b**) Raveling

Figure 8. Porous pavement diseases.

According to the China industrial standards "*Highway Performance Assessment Standards*" (JTG5210-2018), the values of the indicators DR, RD, IRI, and SFC were converted into the PCI, RDI, RQI, and SRI, which were illustreated by Figures 9–11.

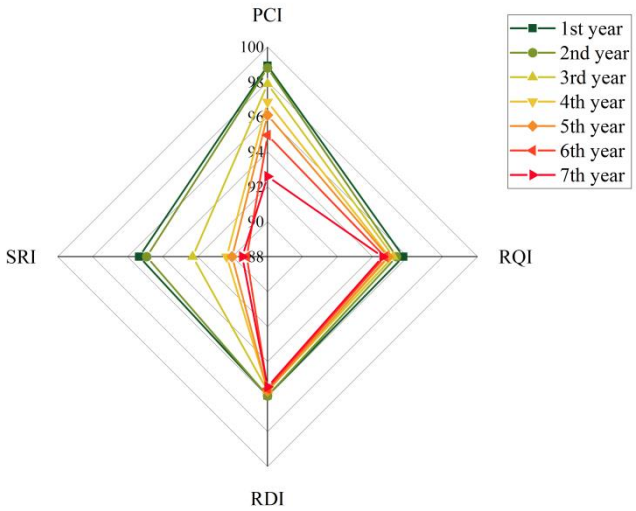

Figure 9. PUC-10 pavement service performance scores.

Preprints (www.preprints.org) | NOT PEER-REVIEWED | Posted: 7 December 2023 doi:10.20944/preprints202312.0490.v1

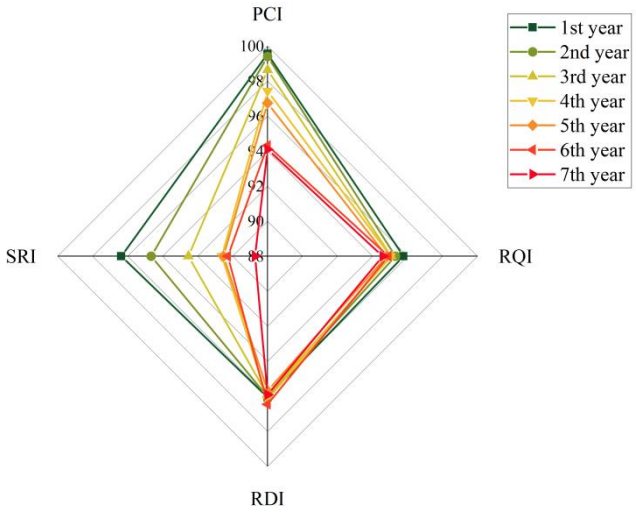

Figure 10. PAC-13 pavement service performance scores.

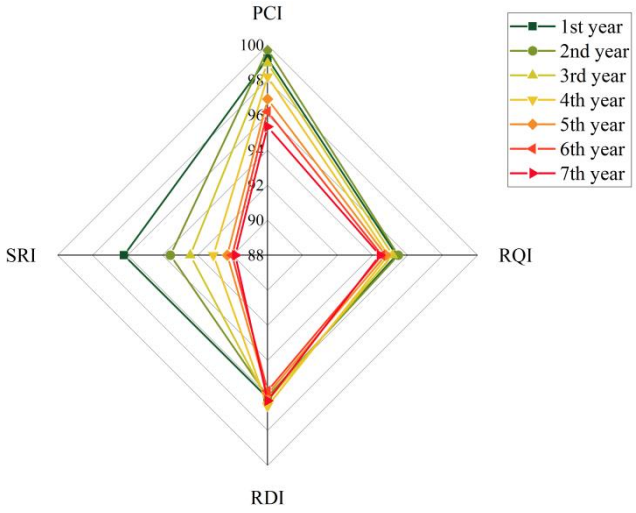

Figure 11. PUC-10+PAC-13 pavement service performance scores.

During the 1-7 years of operation, the service performance of the porous asphalt pavement declined to a certain extent, among which the PCI and SRI show the most notable decrease. The PCI of the three porous pavement structures dropped to 92.59-95.34, and the attenuation rate reached 3.93%-6.41% compared with that in the first year of operation. This is because the porous asphalt pavement has a higher connected porosity, and asphalt has larger contact area with the external environment, such as pores and water. Compared with the dense pavement surface, asphalt mixtures are more susceptible to aging and water damage, and its crack disease develops faster, resulting in a greater decrease of PCI. During the 1-7 years of operation, the SRI of the three porous pavement structures decreased to 88.72-89.45, and the attenuation rate reached 6.17%-7.93%, which may be affected by factors such as aggregate angularity and polishing value [35,36]. Under the repeated action of vehicle load, the micro-texture of the coarse aggregate reduced, resulting in a decrease of the skid-resistance property. RQI of the three porous pavement structures was reduced to 94.42-94.58, with a attenuation rate of 0.99%-1.24%, and the RDI dropped to 95.45-96.31, with a attenuation rate within 0.6%, which is due to the porous asphalt mixture had a skeleton-pore structure, and the coarse aggregates were embedded with each other, the pavement shows better resistance to deformation, so the RQI and RDI did not decay significantly after 7 years of operation.

Preprints (www.preprints.org) | NOT PEER-REVIEWED | Posted: 7 December 2023 doi:10.20944/preprints202312.0490.v1

As the age increases, the anti-cracking performance and skid-resistance of porous asphalt pavement significantly decrease. It can be found that in order to improve the durability of porous asphalt pavement, it is necessary to control the development of transverse cracks and to improve the skid-resistance performance.

3.2. Tire/Pavement Noise Analysis Based on the OBSI Method

To quantify tire/pavement noise of the porous asphalt, the OBSI test was carried out on porous asphalt pavement on different lanes with a length of 5 km. The test speeds were 80 km/h and 100 km/h respectively, and the test results are shown in Figure 12.

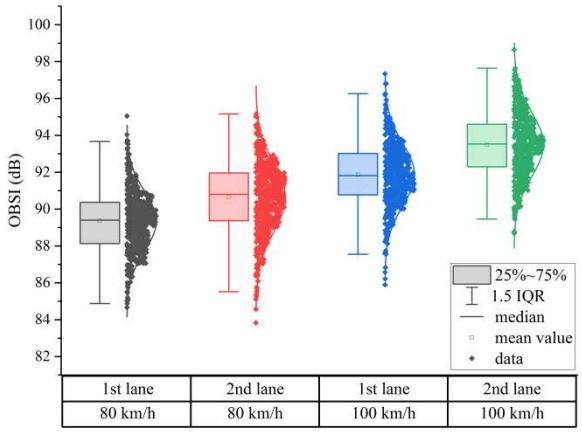

Figure 12. OBSI of each lane at different test speeds.

According to Figure 12, at the test speed of 100 km/h, the average OBSI values of the noise of the first and second lanes were 91.86 dB and 93.50 dB, respectively, which were remarkably higher than those at the test speed of 80 km/h (89.35 dB and 90.63 dB). At the test speed of 100 km/h, the average OBSI value of the first lane was increased by 2.51 dB compared with that at 80 km/h, while that of the second lane was increased by 2.87 dB. It indicates that the OBSI is greatly impacted by the test speed; the faster the drving speed is, the greater the OBSI value will be. At the same speed, the average OBSI value of the second lane was 1.64 dB (100 km/h) and 1.28 dB (80 km/h) higher than that of the first lane, respectively, suggesting that the OBSI value of the second lane was slightly greater than that of the first lane at the same test speed. Based on the box plot, the interquartile spacing [3/4 quantile (75% quantile value) - 1/4 quantile (25% quantile value)] of the second lane was slightly greater than that of the first lane. It means that the OBSI dispersion of the second lane was greater than that of the first lane, which may be caused by the pavement condition indicators of each lane.

To understand the influence of different lanes on the pavement condition indicators, the distribution statistics of the test data of the SMTD, RD, DR, IRI, and SFC corresponding to the tested section by the OBSI with a length of 5 km were carried out. The results are shown in Figure 13. It was revealed that the average values of SMTD and SFC of the first lane were higher than those of the second lane, RD and IRI were lower than those of the second lane, and the DR values of the two lanes were basically 0. It suggests that the service performance of the pavement of the two lanes is satisfactory, and the service performance of the first lane of the pavement is better than that of the second lane. The average IRI value of the two lanes was slightly greater than the median, and the quantile spacing of 75-95% was much greater than that of 5-25%, indicating that there were more points with large IRI values, which may be one of the main causes of tire/pavement noise. Therefore, the pavement condition indicators of different lanes are different, and the poor service performance of the pavement is one of the main reasons for the greater noise levels.

To clarify the influence law of different pavement structures on OBSI, the OBSI test data with a length of 5 km were classified by different pavement structures, as shown in Figure 14. It was manifested that under the same test conditions, the OBSI noise level of the three porous pavement

Preprints (www.preprints.org) | NOT PEER-REVIEWED | Posted: 7 December 2023 doi:10.20944/preprints202312.0490.v1

structures was greatly lower than that of the dense gradation pavement. The three porous pavement structures had better noise reduction characteristics. Compared with ECA, their OBSI noise could be reduced by 2.09 dB, 1.53 dB, and 2.88 dB, respectively. PUC+PAC had the best noise reduction effect compared to the other two porous pavement structures, with an average OBSI value of 91.23 dB. This is because it has a two-layer porous asphalt structure, and the connected pores are not easily blocked by the dust during the pavement service, bringing a more durable noise reduction effect. The OBSI of the PAC-13 pavement structure was slightly higher than that of the PUC-10 pavement, and its standard deviation and interquartile spacing were higher than those of the other two pavement structures. It implies that the greater dispersion of OBSI values is possibly due to the influence factors such as connected porosity and pavement service performance during service.

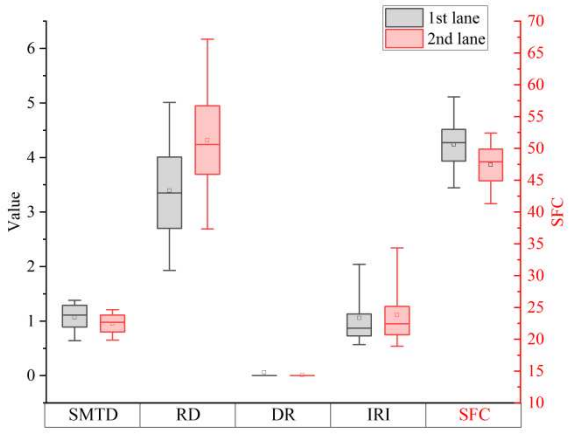

Figure 13. Distribution of pavement condition indicators in different lanes.

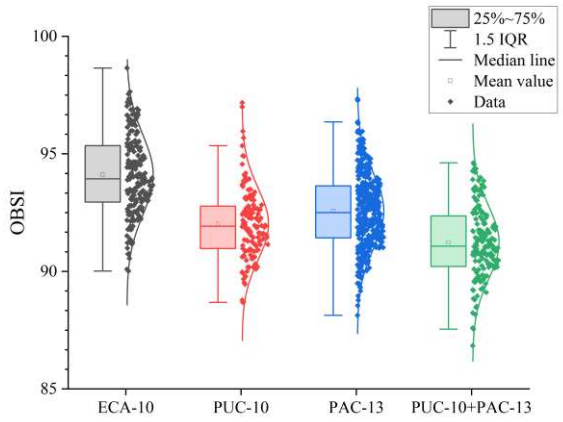

Figure 14. OBSI distribution in different pavement structures.

3.3. Correlation Analysis on OBSI and Pavement Performance Indicators

The test data were classified according to OBSI test speeds (100 km/h and 80 km/h), forms of pavement structure, and lanes. Table 3 shows the classification variables settings, and Table 4 presents the Pearson linear correlation analysis results.

Table 3. Variable settings for the linear regression model.

Variable	Variable setting
Test speed	1=80 km/h; 2=100 km/h
Lane	Passing lane=1; Driving lane =2

Preprints (www.preprints.org) | NOT PEER-REVIEWED | Posted: 7 December 2023 doi:10.20944/preprints202312.0490.v1

Pavement structure	1= Compact gradation pavement; 2=PUC-10; 3=PAC-13; 4=PUC-10+PAC-13
Type of pavement disease	1= No damage; 2= Transverse cracks; 3= Longitudinal cracks; 4= Repair

Table 4. Correlation analysis between OBSI and the indicators (n=2280).

Indicator		*M (SD)*	Range	OBSI	Speed	Lane	Pavement structure	Pavement disease
OBSI (dB)	Correlation significant	91.33 (2.30)	83.83-98.65	1				
Speed (km/h)	Correlation significant	-	-	0.585* 0.000	1			
Lane	Correlation significant	-	-	0.317* 0.000	0.000 1.000	1		
Pavement Structure	Correlation significant	-	-	-0.201* 0.000	0.000 1.000	0.161* 0.000	1	
Pavement disease	Correlation significant	-		0.034 0.109	0.003 0.899	0.036 0.089	-0.195* 0.000	1

*Correlation is significant at a confidence level (two-measure) of 0.01.

A hypothesis test on the correlation coefficient between OBSI and speed was conducted, with $p<0.01$ and the test level $\alpha=0.01$ adopted. The result rejected the null hypothesis. It was considered that the regression coefficient was significantly different from 0, there was a significant linear relationship between OBSI and speed, with a correlation coefficient of 0.585. The $p<0.01$ indicated that the linear relationship between OBSI and Lane was significant, and the correlation coefficient was 0.317. The $p<0.01$ suggested a significant linear relationship between OBSI and pavement structure, and the correlation coefficient was -0.201. The $p>0.01$ manifested that there was no significant correlation between OBSI and pavement disease.

In summary, OBSI had significant correlations with speed, lane, and pavement structure, consistent with the analysis results in Figures 12–14. The correlation between OBSI and pavement disease was not significant, mainly due to the few diseased sections in the tested section and the lack of sufficient diseased section data to support the correlation analysis between OBSI and pavement disease.

To clarify the correlation between the pavement performance indicators and tire/pavement noise intensity with porous pavement structures, the correlation analysis was carried out on the OBSI at the test speed of 100 km/h, and the SMTD, RD, DR, SFC, and IRI of different pavement structures. The test results are shown in Table 5.

Table 5. Correlation analysis of OBSI and various indicators of different pavement structures.

Pavement structure	Indicator	SMTD	RD	DR	SFC	IRI
ECA-10	Correlation	0.567*	0.035	-0.123	-0.304*	-0.121
	Significance	0.000	0.619	0.083	0.000	0.088
PUC-10	Correlation	0.265	0.545*	0.084	0.132	-0.089
	Significance	0.157	0.002	0.738	0.488	0.638
PAC-13	Correlation	0.127	-0.135	0.074	0.082	0.022
	Significance	0.067	0.052	0.486	0.240	0.746
PUC-10+PAC-13	Correlation	-0.052	-0.024	0.142	-0.231*	-0.044
	Significance	0.554	0.786	0.095	0.008	0.618

*Correlation is significant at a confidence level (two-measure) of 0.01.

 doi:10.20944/preprints202312.0490.v1

According to Table 5, the OBSI noise values of various pavement structures had a significant linear correlation with pavement performance indicators. The $p<0.01$ for OBSI noise levels of ECA compact gradation asphalt pavement with SMTD and SFC revealed that the OBSI noise value of ECA compact gradation asphalt pavement had a significant linear relationship with SMTD and SFC, and the correlation coefficients r were 0.567 and -0.304, respectively. The SMTD and SFC had a significant impact on the OBSI noise of ECA compact gradation asphalt pavement due to the small porosity of ECA, causing a direct correlation between noise values and SMTD. Besides, SMTD is a macroscopic texture that has a certain impact on the skid-resistance performance of the pavement, so both SMTD and SFC are closely associated with the OBSI value. The $p<0.01$ for the OBSI noise value of PUC-10 porous asphalt pavement and RD denoted that the OBSI noise values of PUC-10 porous asphalt pavement had a significant linear relationship to RD, with a correlation coefficient r of 0.545. It suggests that compared with other pavement condition indicators, the RD has a more significant impact on the OBSI noise value of PUC-10 porous asphalt pavement. The reason is that the PUC-10 structural layer is thinner, and the rutting of the section compresses the pores of PUC-10, leading to the decreased noise absorption performance and the increased OBSI value, so the OBSI value has a significant linear relationship with the RD. There was no obvious linear correlation between the OBSI noise value of PAC-13 porous asphalt pavement and SMTD, RD, DR, SFC, and IRI, and the correlation coefficients r were all less than 0.2. PAC-13, due to its high porosity, is affected by the blocking of the pores during service; both the reduction of noise absorption performance of the pavement and the decrease of air pump noise affect the tire/pavement noise value, which may lead to a weaker correlation between the OBSI noise value and pavement condition indicators. The $p<0.01$ for the OBSI noise value of PUC-10+PAC-13 porous asphalt pavement with SFC indicated a significant linear relationship between the OBSI noise value and SFC, with a correlation coefficient of -0.231. Under the influences of loading and environmental factors on the pavement, some microscopic texture is changed [37–39], which improves the tire/pavement noise value at high-frequency range. Also, the microscopic wear of the pavement will directly affect the skid-resistance performance of the pavement (SFC decline). Therefore, the OBSI noise value has a negative correlation with the SFC.

As a result, the sensitivity of tire/pavement noise of different pavement structures to each pavement condition indicator varies. According to the data analysis, the section tracked and observed on this study had no serious disease, with the largest proportion of transverse cracks. The transverse crack disease may not significantly impact on tire/pavement noise, which may lead to an insignificant correlation between DR and OBSI. The impact of disease types, especially raveling, on noise should be focused on for future studies on porous asphalt tire/pavement noise.

4. Conclusions

In this study, the medium-term performances of different porous asphalt pavement structures were analyzed, and the tire/pavement noise levels of three types of porous pavement structures (PUC-10, PAC-13, and PUC-10+PAC-13) in service was measured. The correlation between OBSI and various pavement condition indicators was analyzed. The conclusions achieved are as follows:

(1) The DR and SFC of the three porous asphalt pavements decayed significantly with the increased age of the pavement, while the IRI and RD exhibited no remarkable decline. SFC had a relatively obvious decline in 1-4 years of operation, with a decrease rate of 13.8-17.0%. During the 3-7 years of operation, the transverse cracks of porous asphalt pavement developed rapidly, which was the main disease type of porous asphalt pavement at this moment.

(2) The OBSI was significantly correlated with SFC, IRI, OBSI test speed, tested lane, and the forms of pavement structure. The OBSI testing speeds, different lanes, and the types of pavement structures greatly influenced the OBSI noise value. This is because different lanes and pavement structures have different pavement performance due to environmental and loading effects, resulting in different noise levels.

(3) The three porous pavement structures (PUC-10, PAC-13, and PUC-10+PAC-13) had better noise reduction characteristics compared with the noise of compact gradation pavement. Two-layer porous asphalt pavement had the best noise reduction effect compared to the other two porous

pavement structures for medium-term service. Beause the connected pores of two-layer porous asphalt mixture are not easily blocked by the dust during the pavement service, bringing a more durable noise reduction effect.

(4) The OBSI noise value of the ECA compact gradation asphalt pavement had a significant linear relationship with the SMTD and SFC. Compared with other pavement condition indicators, the RD had a more significant effect on the OBSI noise value of the PUC-10 porous asphalt pavement. The linear relationship between the OBSI noise value of PUC-10+PAC-13 porous asphalt pavement and SFC was significant. Under the influences of loading and environmental factors on the pavement, some microscopic texture is changed, which improves the tire/pavement noise value at high-frequency range. Also, the microscopic wear of the pavement will directly affect the skid-resistance performance of the pavement.

There was no serious disease in the porous asphalt section based on the medium-term investigaton, and the proportion of transverse cracks was the main types of disease. The transverse crack has little impact on tire/pavement noise. Emphasis should be attached to the effect of disease types, especially the raveling on porous asphalt tire/pavement noise, in order to establish the relationship between tire/pavement noise and pavement disease.

Author Contributions: Hao Wu: Data curation, Visualization, Investigation, Writing—Original draft; Ge Wang: Funding acquisition, Project administration; Mingliang Li: Formal analysis, Writing - review & editing; Yue Zhao: Funding acquisition, Project administration; Jun Li: Writing—Reviewing and Editing, Validation; Dingding Han: Writing - review & editing, Investigation, Data curation. Pengfei Li: Formal analysis, Writing - review & editing, Investigation. All authors have read and agreed to the published version of the manuscript.

Funding: General Projects of Beijing Natural Science Foundation (No. 8232015). Pilot Project of Research Institute of Highway Ministry of Transport (No. QG2021-1-4-5). Research on the Life-Cycle Maintenance Strategy of Porous Asphalt Pavement by Research Project of Jiangsu Communications Holding Company .

Institutional Review Board Statement: Not applicable.

Informed Consent Statement: Not applicable.

Data Availability Statement: Not applicable.

Acknowledgments: The authors would like to thank the reviewers for their comments on this paper.

Conflicts of Interest: The authors declare no conflict of interest

References

1. Stempihar, J.J.; Pourshams, M.T.; Kaloush, K.E.; Rodezno, M.C. Porous Asphalt Pavement Temperature Effects for Urban Heat Island Analysis. *Transportation Research Record: Journal of the Transportation Research Board*. **2012**, 2293, 123-130.
2. Michiyuki, Y.; Hiroshi, N.; Takuya, M. Sound absorption mechanism of porous asphalt pavement. *Journal of Ince/japan*. **1999**, 25, 29-43.
3. Schaus, L.; Tighe, S.L.; Uzarowski, L. Porous Asphalt Pavement Designs: Canadian Climate Use. *Transportation Research Board Meeting.* **2008.**
4. Pakholak, R.; Plewa, A.; Gardziejczyk, W. Influence of Type of Modified Binder on Stiffness and Rutting Resistance of Low-Noise Asphalt Mixtures. *Materials (Basel)*. **2021**, 14, 2884.
5. Rassoshenko, I.; Nikitenko, A.; Ivanov, N. Low-Noise Asphalt Application and Its Efficiency Analysis. *Akustika*. **2019**. 34, 127-131.
6. Mo, L.T.; Huurman, M.; Woldekidan, M.F.; Wu, S.P.; Molenaar, A. Investigation into material optimization and development for improved ravelling resistant porous asphalt concrete. *Materials & Design*. **2010**, 31, 3194-3206.
7. Hauwermeiren, W.V.; David, J.; Dekoninck, L. Assessing Road Pavement Quality Based on Opportunistic In-car Sound and Vibration Monitoring. *International Congress on Sound and Vibration.* **2019**.
8. Awwal, A.; Mashros, N.; Hasan, S.A.; Hassan, N.A.; Rahman, R. Road Traffic Noise for Asphalt and Concrete Pavement. *IOP Conference Series Materials Science and Engineering*. **2021**, 1144, 012082.

9. Vaitkus, A.; Skrodenis, D.; Ernas, O.; Vorobjovas, V. Surface Texture And Layer Permeability Of Aquaplaning Resistant Asphalt Pavements. *IOP Conference Series: Materials Science and Engineering*. **2021**, 1202, 012026.
10. Li, M.; Lu, H.; Li, J.; Mao, Q.; Chen, L. Performance study and application of porous ultra-thin wearing course for asphalt pavement maintenance. *IOP Conference Series: Materials Science and Engineering*. **2021**, 1075, 012014.
11. Rita Kleizien, O.S.; Simanavitiene AVaR. Asphalt Pavement Acoustic Performance Model. *Sustainability*. **2019**, 11, 2938.
12. Pizzo, L.; Bianco, F.; Moro, A.; Schiaffino, G.; Licitra, G. Relationship between tyre cavity noise and road surface characteristics on low-noise pavements. *Transportation Research Part D Transport and Environment*. **2021**, 98, 102971.
13. Spies, L.; Li, T.; Burdisso, R.; Sandu, C. An artificial neural network (ANN) approach to model Tire-Pavement interaction noise (TPIN) based on tire noise separation. *Applied Acoustics.* **2023**, 206, 109294.
14. Shen, D.H.; Wu, C.M.; Du, J.C. Application of Grey Model to Predict Acoustical Properties and Tire/Road Noise on Asphalt Pavement. *IEEE Intelligent Transportation Systems Conference*. **2006**.
15. Faßbender, S.; Oeser, M. Investigation on an Absorbing Layer Suitable for a Noise-Reducing Two-Layer Pavement. *Materials* **2020**, 13, 1235.
16. Zhang, H.; Liu, Z.; Meng, X. Noise reduction characteristics of asphalt pavement based on indoor simulation tests. *Construction and Building Materials*. **2019**. 215(AUG.10): 285-297.
17. Jin, D.; Ge, D.; Wang, J.; Malburg, L.; You, Z. Reconstruction of Asphalt Pavements with Crumb Rubber Modified Asphalt Mixture in Cold Region: Material Characterization, Construction, and Performance. *Materials*. **2023**, 16, 1874.
18. Jaskula, P.; Ejsmont, J.A.; Gardziejczyk, W.; Mioduszewski, P.; Stienss, M.; Motylewicz, M.; Szydlowski, C.; Gierasimiuk, P.; Rys, D.; Wasilewska, M. Bitumen-Based Poroelastic Pavements: Successful Improvements and Remaining Issues. *Materials.* **2023**, 16, 983.
19. Chu, L.; Tan, K.H.; Fwa, T.F. Evaluation of wearing course mix designs on sound absorption improvement of porous asphalt pavement. *Construction and Building Materials*. **2017**, 141, 402-409.
20. Gao, L.; Wang, Z.; Xie, J.; Wang, Z.; Li, H. Study on the sound absorption coefficient model for porous asphalt pavements based on a CT scanning technique. *Construction and Building Materials*. **2020**, 230, 117019.
21. Mahmud, M., Hassan, N.A.; Hainin, M.R.; Che, R.I.; Mashros, N. Characterisation of microstructural and sound absorption properties of porous asphalt subjected to progressive clogging. *Construction and Building Materials*. **2021**, 283, 122654.
22. Ni. T.Y.; Jiang, C.H.; Tai, H.X.; Zhao, G.Q. Experimental Study on Sound Absorption Property of Porous Concrete Pavement Layer. *Applied Mechanics and Materials*. **2014,** 507, 238-241.
23. Zhang, Y.; Li, H.; Abdelhady, A.; Du, H. Laboratorial investigation on sound absorption property of porous concrete with different mixtures. *Construction and Building Materials*. **2020**, 259, 120414.
24. Xu, B. Li, M.; Liu, S.; Fang, J.; Ding, R.; Cao, D. Performance analysis of different type preventive maintenance materials for porous asphalt based on high viscosity modified asphalt. *Construction and Building Materials*. **2018**, 191, 320-329.
25. Zw, A.; Jx, A.; Lei, G.A.; Ml, B.; Yl, A. Improvement of acoustic model and structural optimization design of porous asphalt concrete based on meso-structure research. *Construction and Building Materials*. **2020**, 265, 120327.
26. Chen, D.; Ling, C.; Wang, T.; Su, Q.; Ye, A. Prediction of tire-pavement noise of porous asphalt mixture based on mixture surface texture level and distributions. *Construction and Building Materials*. **2018**, 173, 801-810.
27. Alber, S.; Ressel,W.; Liu, P.; Wang, D.; Oeser, M. Influence of soiling phenomena on air-void microstructure and acoustic performance of porous asphalt pavement. *Construction and Building Materials*. **2018**, 158, 938-948
28. Amrina, R.J.A.; Buchari, E. Evaluation Pavement Deteriorating Condition on Surface Distress Index (SDI) Data Using Radial Basis Function Neural Networks (RBFNN). *Journal of Physics: Conference Series*, **2019**, 032008.
29. Hao, W.; Wang, Z.; Evaluation of pavement surface friction subject to various pavement preservation treatments. *Construction & Building Materials.* **2013**, 48, 194-202.

30. Afarin, K.; Amir, G. Machine learning for developing a pavement condition index. *Automation in Construction*. **2022**, 139, 104296.
31. Piryonesi, S.M.; Tamer, E.; Examining the relationship between two road performance indicators: Pavement condition index and international roughness index. *Transportation Geotechnics*. **2021**, 100441.
32. Cao, L.; Li, L.W.; Yang, C.; Zhang, B.; Dong, Z. Performance prediction of expressway pavement in high maintenance level areas based on cosine deterioration equation: A case study of Zhejiang Province in China. *Journal of Road Engineering*. **2022**, 267-278.
33. Vaitkus, A.; Cygas, D.; Motiejunas, A.; Pakalnis, A.; Miskinis, D. Improvement of road pavement maintenance models and technologies. *Baltic Journal of Road & Bridge Engineering*. **2016**, 11, 242-249.
34. Ganji, MR.; Golroo, A.; Sheikhzadeh, H.; Ghelmani, A.; Bidgoli, MA. Dense-graded asphalt pavement macrotexture measurement using tire/road noise monitoring. *Automation in Construction*. **2019**, 106, 102887.
35. Lei J., Zheng N., Chen X.,et al; Research on the relationship between anti-skid performance and various aggregate micro texture based on laser scanning confocal microscope. *Construction and Building Materials*. **2022**, 125984.
36. Zheng N, Bi J, Dong S, Lei J., He Y., Cui Z., Chen L.; Testing and evaluation for long-term skid resistance of asphalt pavement composite seal using texture characteristics. *Construction and Building Materials*. **2022**, 129241
37. Víctor, V.; Fernando, T.; Pedro, H.; Santiago, P. Surface Aging Effect on Tire/Pavement Noise Medium-Term Evolution in a Medium-Size City. *Coatings*. **2018**, 8, 206.
38. Cedric, V.; Anneleen, B.; Barbara, V. The Acoustical Durability of Thin Noise Reducing Asphalt Layers. *Coatings*. **2016**, 6, 21.
39. Li, M.; Van, K.W.; Ceylan, H.; Tang, G.; Martin, V.D.V.; Molenaar, A. Influence of road surface characteristics on tire–road noise for thin-layer surfacings. *Journal of Transportation Engineering*, **2015**, 141, 04015024.